Article

J. Biol. Regul. Homeost. Agents. 2024; 38(6): 5305–5316
https://doi.org/10.23812/j.biol.regul.homeost.agents.20243806.424

Binimetinib Attenuates Skin Fibrosis by Inhibiting the TGF-β1 Signaling Pathway

Ruiqi Shen[1], Xiaohe Li[2], Honggang Zhou[2], Litao Zhang[3,*]

[1]Graduate School, Tianjin Medical University, 300070 Tianjin, China
[2]State Key Laboratory of Medicinal Chemical Biology, College of Pharmacy and Tianjin Key Laboratory of Molecular Drug Research, Nankai University, Haihe Education Park, 300353 Tianjin, China
[3]Department of Dermatology, Tianjin Academy of Traditional Chinese Medicine Affiliated Hospital, 300120 Tianjin, China
*Correspondence: zhanglitao@medmail.com.cn (Litao Zhang)
Submitted: 17 March 2024 Revised: 24 April 2024 Accepted: 29 April 2024 Published: 1 June 2024

Background: Dermatofibrosis diseases (e.g., keloids) are abnormal pathological results of the tissue healing process. They are characterized by the excessive proliferation of fibroblasts in the dermis and the excessive deposition of extracellular matrix. Existing treatments for dermatofibrosis have not achieved satisfactory results. The therapeutic efficacy of Binimetinib as a clinical agent for treating cutaneous malignancies in the field of fibrosis has not been extensively studied. Therefore, this study aims to investigate the antifibrotic activity of Binimetinib both *in vitro* and *in vivo* against dermal fibrosis, as well as elucidate its underlying mechanism.

Methods: In this study, we explored the potential effects and underlying mechanisms of Binimetinib on dermal fibrosis both *in vitro* and *in vivo*. In the *in vitro* experiments, we applied the Cell Counting Kit-8 (CCK-8) assay, wound healing assay, and western blotting to examine the inhibitory effects of Binimetinib on the proliferation, migration, and activation of mouse primary dermal fibroblasts (PSFs) and human keloid fibroblasts (KFs). In the *in vivo* experiments, we established a bleomycin mouse dermal fibrosis model and a nude mouse subcutaneous keloid model to verify the inhibitory effect of Binimetinib on dermal thickening in bleomycin model mice and on growth in subcutaneous keloid model in nude mice. Additionally, we investigated the expressions of proteins related to the transforming growth factor-β1 (TGF-β1) signaling pathway.

Results: *In vitro* experiments showed that Binimetinib effectively suppressed the proliferation, migration, and activation of KFs and PSFs in a dose-dependent manner ($p < 0.05$). *In vivo* experiments revealed that Binimetinib attenuated dermal thickening induced by bleomycin (BLM), reduced hydroxyproline content, and reduced the expression of fibrosis markers in a bleomycin-induced dermal fibrosis model ($p < 0.05$). Moreover, in a nude mouse subcutaneous keloid model, Binimetinib not only inhibited keloid proliferation and weight gain but also suppressed the expression of fibrosis markers ($p < 0.05$). Further mechanistic studies indicated that Binimetinib inhibited both TGF-β1/recombinant SMAD family member (Smad) signaling and TGF-β1/non-Smad signaling pathways associated with fibrosis ($p < 0.05$).

Conclusions: In summary, our results confirm that Binimetinib effectively suppresses fibrosis both *in vivo* and *in vitro* by inhibiting the TGF pathway, demonstrating significant potential for fibrosis treatment.

Keywords: Binimetinib; skin fibrosis; skin fibroblasts; ERK/Akt/P38 signaling pathway; TGF-β1/Smad signaling pathway

Introduction

Anomalies in tissue repair following deep dermal skin injuries can lead to dermal fibrosis, a pathological condition that can manifest in various forms such as keloids, hyperplastic scars, and the immune disorder scleroderma [1]. Keloids, in particular, are dermatofibrotic disorders that commonly arise after skin injuries, burns, or surgeries, characterized by excessive collagen-based extracellular matrix deposition in the dermis [2]. Similar to benign tumors, keloids exhibit tumor-like hyperplasia extending beyond the original injury site, invading surrounding tissues, and causing functional impairment and disfigurement. Keloid scars tend to reoccur even after surgical excision, and current therapeutic drugs demonstrate unsatisfactory outcomes, marked by significant individual variability and notable side effects [3]. Given these limitations, alternative treatments that are safer and more effective are needed.

Recent research has indicated that keloid formation during tissue repair is primarily caused by the excessive proliferation of fibroblasts, the accumulation of extracellular matrix (ECM), and the infiltration of inflammatory cells [4]. Fibroblasts, in particular, play a key role in wound healing and keloid formation [5,6]. While the exact mechanism of keloid formation remains unknown, previous studies have identified transforming growth factor-β1 (TGF-β1) as the principal regulator among the numerous cell growth

Journal of
BIOLOGICAL REGULATORS
and Homeostatic Agents

factors associated with fibroblast activation in pathological keloid scars [7]. TGF-β1 induces the downstream recombinant SMAD family member (Smad)/non-Smad signaling pathway to promote fibroblast proliferation, activation, and resistance to apoptosis [8]. Furthermore, it sustains keloid growth by facilitating ECM synthesis and deposition, inhibiting collagenase activity, and disrupting the normal collagen degradation process. This suggests that TGF-β1 and related signaling pathways play a crucial role in the fibrotic process. Consequently, targeting the TGF-β1 signaling pathway has emerged as a potential therapeutic approach for dermatofibrotic diseases [9,10]. Binimetinib, a selective mitogen-activated extracellular signal-regylated kinase1/2 (MEK1/2) inhibitor currently used for the treatment of cutaneous melanoma, has been the subject of scientific exploration for its potential effects on various tumors [11,12].

Given the pathological similarities between dermatofibrotic diseases, particularly keloids, and tumors [13], Binimetinib's potential role in the treatment of dermatofibrotic diseases has been investigated in this study, with a focus on fibroblast and TGF-β1-related signaling pathways. *In vitro* experiments verified the inhibitory effect of Binimetinib on the proliferation, migration, and activation of fibroblasts. Two animal models of dermal fibrosis were also established to validate the *in vivo* antifibrotic effects of Binimetinib. Key markers, such as α-smooth muscle actin (α-SMA) for fibroblast activation, collagen I (Col1) for ECM deposition, and fibronectin (Fn) were primarily examined. Additionally, the inhibitory effect of Binimetinib on both TGF-β1/Smad signaling and TGF-β1/non-Smad signaling pathways was tested.

Materials and Methods

Tissue Samples from Human Keloids

The specimens of keloid tissues utilized in this study were obtained from five patients who underwent keloidectomy at the Affiliated Hospital of the Tianjin Institute of Traditional Chinese Medicine. Each human participant involved in this research provided their informed consent preceding their enrollment in the study. Furthermore, the study's methods were approved by the Ethics Committee of Nankai University on December 20th, 2021 (Approval No. NKUIRB2021116), and all experimental protocols strictly adhered to the appropriate guidelines and regulations about human subjects. The principles of the Declaration of Helsinki were observed throughout our experiments.

Keloid Fibroblast Isolation and Culture

The process of isolating and cultivating keloid fibroblasts (KFs) was conducted following a previously established protocol documented in the literature [14]. Keloid tissue samples were removed in a sterile environment and the surrounding epidermal layer and subcutaneous fat were carefully clipped off. The excised specimens were subsequently sectioned into small fragments of approximately 5 cubic millimeters in volume. These fragments were cultured in Dulbecco's Modified Eagle's Medium (DMEM, 11995, Solarbio, Beijing, China) supplemented with 10% Fetal Bovine Serum (FBS, S9030, Solarbio, Beijing, China) and incubated in a constant temperature incubator at 37 °C with 5% CO_2. The isolated cells were morphologically characterized and confirmed as KFs through the expression of the fibrosis marker α-SMA [15]. As the cell population reached confluence, they were passaged at a 1:3 ratio. All cells utilized in this study underwent rigorous testing to ensure they were free from mycoplasma contamination.

Table 1. Reagent information sheet.

Reagent name	Product number	Company	Address
DNASE	D7076	Beyotime	Shanghai, China
Collagenase TypeII	C8150	Solarbio	Beijing, China
DispaseII	CD4691	Coolaber	Beijing, China
Povidone iodine	A606166-0100	BBI	Beijing, China

Primary Dermal Fibroblast Isolation and Culture

The process of isolating and culturing primary dermal fibroblasts (PSFs) from the dermis of neonatal C57BL/6 mice was referenced in the literature [16]. We used 10 C57BL/6 mice within 24 h of birth, weighing 1.5–2.5 g, obtained from Beijing Viton Lihua Laboratory Animal Technology Co. Anesthesia was induced using 100 µL of sodium pentobarbital 60 mg/kg. These cells were cultured in DMEM medium supplemented with 10% FBS and incubated in an incubator at 37 °C and 5% CO_2. The isolated cells were morphologically identified and tested positive for the fibrosis marker Col1, confirming them as PSFs [17]. Upon reaching confluence, the cells were passaged at a 1:3 ratio. All cells used in this study were tested and verified to be free from mycoplasma contamination. Details of the reagents required for the extraction process are provided in Table 1.

Analyzing Cell Viability

Cell viability was assessed using the 3-(4,5-dimethylthiazol-2-yl)-2,5-diphenyltetrazolium bromide (MTT) assay (M1020, Solarbio, Beijing, China). The compound Binimetinib (T2508, TargetMOI, Shanghai, China) was applied to PSFs in 96-well plates at concentrations ranging from 0 to 80 µM, allowing a 24-hour interaction period. Following this, 10 µL of MTT solution at 5 mg/mL was added to each well and incubated at 37 °C in a light-protected thermostat for 4 h. Subsequently, 150 µL of DMSO was added to each well, and an enzyme labeling instrument (A51119500C, Thermo, Waltham, MA, USA) was used to measure absorbance at 570 nm. The inhibition rate was calculated using the formula: Inhibition rate = [1 – (experimental group – zeroing group)/(Control group – zeroing group)] × 100%.

CCK-8 Assay

The impact of drugs on the proliferation of KFs and PSFs was assessed using the Cell Counting Kit-8 (CCK-8) assay (CA1210, Solarbio, Beijing, China). For this, 96-well plates were inoculated with well-grown KFs or PSFs. The cells were then exposed to varying concentrations of Binimetinib (0, 2.5, 5, 10, and 20 μM). After 24 h, cells were assessed using the CCK-8 reagent. The optical density values of the media in each well were measured at 450 nm using an enzyme labeling instrument. The absorbance data obtained were compared with the mean value of the Control group and then analyzed.

Wound Healing Assay

Twelve-well plates were inoculated with KF or PSF cells. Once the cells had formed a confluent monolayer, a sterile 100 μL pipette tip was used to create a wound in the cell layer. The cells were then treated with Binimetinib, either in the absence or presence of TGF-β1 (10 ng/mL). The wound healing process was observed at 0, 12, 24, 36, and 48 h using an inverted light microscope (65798301370, Phenix, Shangrao, China). For each treatment group, images were captured at three distinct locations within the well. The acquired images were analyzed using ImageJ (V1.8.0, NIH, Bethesda, MD, USA) software. The wound width was measured, and the data were compared to the initial measurements taken on Day 0.

Quantitative Real-Time Polymerase Chain Reaction (qRT-PCR)

All qRT-PCR experiments were performed using β-Actin or glyceraldehyde-3-phosphate dehydrogenase (*GAPDH*) as endogenous reference genes. The gene expression of the target genes relative to the endogenous reference genes was quantified using the Livak method ($2^{-\Delta\Delta Ct}$ method). RNA was extracted using the TRIzol reagent (R1100, Solarbio, Beijing, China). The extracted RNA was then reverse-transcribed. We used a real-time fluorescence quantitative PCR instrument (Lightcycler480, Roche, Mannheim, Germany) to obtain the data. Subsequent steps were performed according to the primer kit instructions. The primer sequences used in the experiments are presented in Table 2.

Table 2. mRNA primer sequence list.

Gene	Primer	Sequence (5′–3′)
M-*GAPDH*	Forward	AGGTCGGTGTGAACGGATTTG
	Reverse	TGTAGACCATGTAGTTGAGGTCA
M-α-*SMA*	Forward	GCTGGTGATGATGCTCCCA
	Reverse	GCCCATTCCAACCATTACTCC
M-*Col1*α*1*	Forward	CCAAGAAGACATCCCTGAAGTCA
	Reverse	TGCACGTCATCGCACACA
M-*Fn*	Forward	GTGTAGCACAACTTCCAATTACGAA
	Reverse	GGAATTTCCGCCTCGAGTCT
H-β-*actin*	Forward	AGGCCAACCGTGAAAAGATG
	Reverse	AGAGCATAGCCCTCGTAGATGG
H-α-*SMA*	Forward	TGGGTGAACTCCATCGCTGTA
	Reverse	GTCGAATGCAACAAGGAAGCC
H-*Col1*α*1*	Forward	AAGCCGGAGGACAACCTTTTA
	Reverse	GCGAAGAGAATGACCAGATCC
H-*Col3*α*1*	Forward	TGGTGTTGGAGCCGCTGCCA
	Reverse	CTCAGCACTAGAATCTGTCC
H-*Fn*	Forward	GCCACTGGAGGTCTTTACCACA
	Reverse	CCTCGGTGTTGTAAGGTGGA

GAPDH, glyceraldehyde-3-phosphate dehydrogenase; α-*SMA*, α-smooth muscle actin; *Col1*α*1*, collagen1α1; *Fn*, fibronectin; *Col3*α*1*, collagen3α1.

Western Blot

The protein samples used in this study were extracted from cells or animal tissues, following the protocols outlined in the literature [18]. The total protein samples were then separated by gel electrophoresis and transferred to polyvinylidene difluoride (PVDF) membranes (IEVH00005, Millipore, Billerica, MA, USA). After blocking the non-specific binding sites, immunoblotting was performed using primary antibodies diluted 1000-fold in skimmed milk (N7861, Lablead, Beijing, China). The membranes were then incubated with horseradish peroxidase (HRP)-conjugated secondary antibody (S0001, Affinity, Cincinnati, OH, USA), and the protein bands were visualized using an ECL (enhanced chemiluminescence) system provided by Affinity Bioscience (KF8003, Affinity, Cincinnati, OH, USA). The images were analyzed using ImageJ software (V1.8.0, NIH, Bethesda, MD, USA). The details of the primary antibodies used in this study are provided in Table 3.

Animals

A total of 68 mice were used in the study, including 23 female nude BALB/c mice aged 6 weeks, weighing 20–22 g, 35 male C57BL/6 mice aged 6–8 weeks, weighing 22–24 g, and 10 C57BL/6 mice less than 24 hours old, weighing 1.5–2.5 g. These mice were purchased from Beijing Viton Lihua Laboratory Animal Technology Co. The animal experiments were conducted with approval from the Institutional Animal Care and Use Committee (IACUC) of Nankai University, under approval number SYXK 2019-0001. For tissue sample collection, the mice were anesthetized with 100 μL 60 mg/kg sodium pentobarbital, followed by cervical dislocation, and the samples were then collected.

Bleomycin-Induced Dermal Fibrosis Model

The backs of C57BL/6 mice were shaved to expose the skin. Dermal fibrosis was induced by intradermal injection of bleomycin (BLM) sulfate (100 μL at a concentration of 500 μg/mL), administered daily for 3 weeks at a single site in their backs [14]. A total of 35 mice were ran-

Journal of
BIOLOGICAL REGULATORS
and Homeostatic Agents

Table 3. Western blot antibody information.

Antibodies	Product number	Company	Address
Collagen I	AF7001	Affinity	Cincinnati, OH, USA
α-SMA	AF1032	Affinity	Cincinnati, OH, USA
Fibronectin	AF0738	Affinity	Cincinnati, OH, USA
P-Smad2	AF3449	Affinity	Cincinnati, OH, USA
Smad2	AF6449	Affinity	Cincinnati, OH, USA
P-Smad3	AF8315	Affinity	Cincinnati, OH, USA
Smad3	AF6362	Affinity	Cincinnati, OH, USA
P-Akt	AF3318	Affinity	Cincinnati, OH, USA
Akt	AF6318	Affinity	Cincinnati, OH, USA
P-ERK	AF1015	Affinity	Cincinnati, OH, USA
ERK	AF0155	Affinity	Cincinnati, OH, USA
P-P38	AF4001	Affinity	Cincinnati, OH, USA
P38	AF6456	Affinity	Cincinnati, OH, USA
β-tubulin	AF7011	Affinity	Cincinnati, OH, USA
GAPDH	AF7021	Affinity	Cincinnati, OH, USA

Smad, recombinant SMAD family member; Akt, protein kinase B; ERK, extracellular regulated protein kinases; P38, P38 mitogen-activated protein kinase.

domly allocated into five groups using a random number table method: (1) NaCl group, which received intradermal injection of carrier solution (100 µL of sterile saline + 1% dimethyl sulfoxide); (2) BLM group, which received intradermal injection of 100 µL of BLM sulfate; and (3–5) treatment groups, which received intradermal injection of 100 µL of BLM combined with Binimetinib at concentrations of 5, 10, and 20 µM. Following the injections, samples were subjected to hematoxylin and eosin (H&E) staining (G1120, Solarbio, Beijing, China) and Masson staining (G1340, Solarbio, Beijing, China). Additionally, skin tissue thickness and hydroxyproline content were measured to evaluate the effects of the treatments.

Subcutaneous Keloid Model in Nude Mice

This modeling methodology is based on literature [19]. Two BALB/c female nude mice were subcutaneously injected on the left dorsal side with 1×10^6 KFs to allow growth to 2000 mm^3. Subsequently, the resulting lump from one mouse was divided equally into 15 parts and placed under the skin on the left side of the back of each of the 15 nude rats. Following this, 21 nude mice were selected and randomly divided into three groups using a random number table method. Once the keloid had reached approximately 100 mm^3, the keloid was administered according to the regimen of 50 µL/100 mm^3 for 7 days, with the groups as follows: (1) seven nude mice in the saline group, (2) seven nude mice receiving Triamcinolone acetonide 4 mg/mL, and (3) seven nude mice receiving Binimetinib 20 µM. The keloid volume was measured every other day during the drug administration period, and the collected data were compared with the initial day's measurements.

Histological Examination

Skin samples were obtained from the dorsal injection site of C57BL/6 mice. The samples were fixed in 10% formaldehyde solution, then dehydrated, embedded, and sectioned at a thickness of 5 µm. The sections were dried, deparaffinized, and stained using hematoxylin and eosin (H&E) as well as Masson's trichrome stain. The stained sections were scanned using an imaging device, and the resulting images were captured and analyzed using ImageJ software.

Immunohistochemical Staining

Tissues removed from mice were fixed, embedded, sectioned (5 µm), and incubated with antibodies against α-SMA (AF1032, Affinity, Cincinnati, OH, USA), collagen I (AF7001, Affinity, Cincinnati, OH, USA), and fibronectin (AF0738, Affinity, Cincinnati, OH, USA) at a 1:200 dilution. The tissue sections were scanned and analyzed using ImageJ software. Immunohistochemical staining kits (KIT-9720, MXB, Fujian, China) were used in these experiments.

Determination of Hydroxyproline Content

The skin samples from C57BL/6 mice, each weighing approximately 10 mg, were carefully separated and placed into individual ampoules. Hydrochloric acid was then added, and the samples were dried at a temperature of 120 °C for approximately 18 h. The resulting mixture was filtered, and the pH was adjusted to a range of 6–8.0. Finally, the solution was diluted with 1× PBS to a total volume of 10 mL. The hydroxyproline (HYP) content within the samples was determined using a hydroxyproline assay kit. The quantitative analysis was performed by measuring the absorbance of the samples at 577 nm.

Statistical Analysis

The experimental data were expressed as mean ± standard deviation (SD). After confirming that the data were normally distributed, statistical analysis was conducted using one-way ANOVA, followed by the Student-Newman-Keuls (S-N-K) post hoc test. Prism (V8.0, GraphPad Software, San Diego, CA, USA) software was used for data processing. A p-value of less than 0.05 was considered statistically significant. The statistically significant levels were denoted as $*p < 0.05$, $**p < 0.01$, $***p < 0.001$, and $****p < 0.0001$.

Results

Binimetinib Inhibits TGF-β1-Induced Proliferation and Migration of Primary Mouse Skin Fibroblasts

Initially, we examined the impact of Binimetinib on the proliferation of primary mouse skin fibroblasts (PSFs) through the MTT assay. The results of the MTT assay revealed that the half maximal inhibitory concentration (IC50) value of Binimetinib in PSFs was 27.16 µM

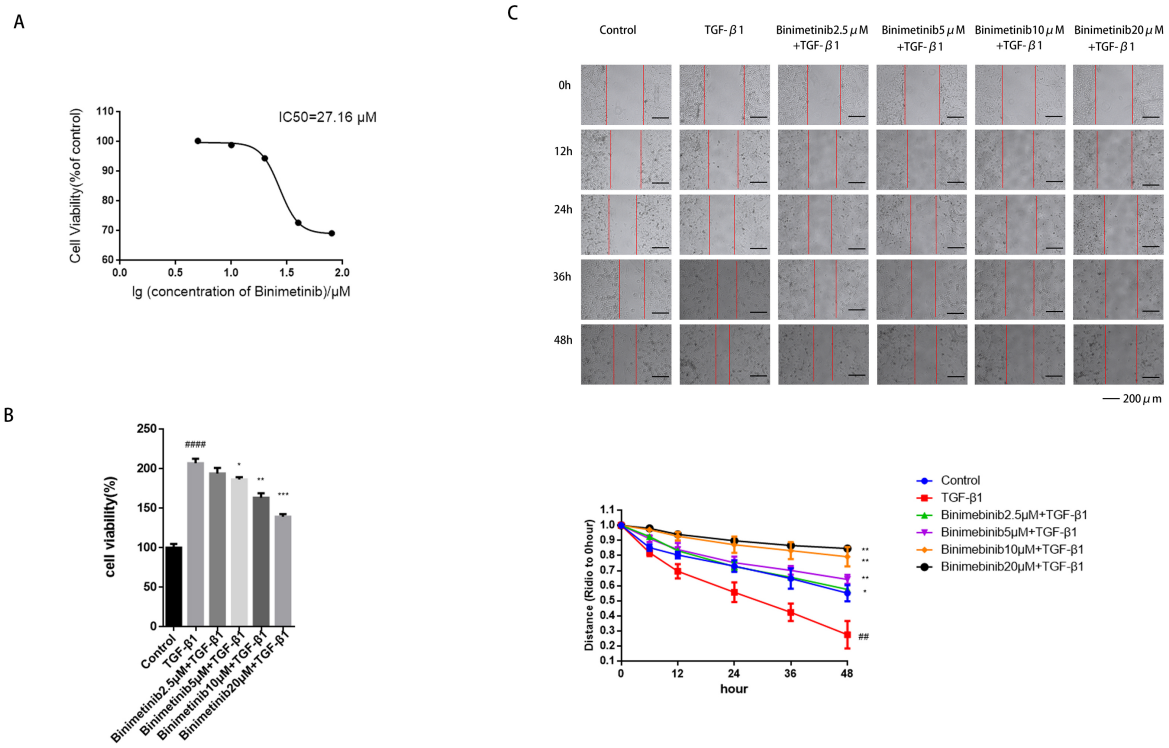

Fig. 1. Binimetinib inhibits the proliferation and migration of PSFs. (A) IC50 = 27.16 μM. (B) Bimetinib inhibited TGF-β1-induced proliferation of PSFs. (C) Effect of bimetinib on TGF-β1 induced migration of PSFs. Results are expressed as mean ± SD (n = 3). $^{\#}$ represents the difference between Control and TGF-β1 groups, $^{\#\#}p < 0.01$, $^{\#\#\#\#}p < 0.0001$, * represents the difference between TGF-β1 and Binimetinib groups, $^{*}p < 0.05$, $^{**}p < 0.01$, $^{***}p < 0.001$. PSFs, primary mouse skin fibroblasts; IC50, half maximal inhibitory concentration; TGF-β1, transforming growth factor-β1; SD, standard deviation.

(Fig. 1A). Additionally, we referred to the effective concentration ranges of Binimetinib in previous studies. Consequently, we selected four concentrations (2.5, 5, 10, and 20 μM) for subsequent pharmacological experiments.

Next, we evaluated the inhibitory effect of Binimetinib on the proliferation of TGF-β1-activated PSFs using the CCK-8 assay. Fig. 1B illustrates that TGF-β1 stimulation accelerated the growth rate of *in vitro*-cultured PSFs ($p < 0.0001$). However, following treatment with Binimetinib, cell proliferation was progressively inhibited in a dose-dependent manner. Notably, the inhibition observed in the Binimetinib 20 μM group was statistically significant ($p < 0.001$). Furthermore, the scratch assay revealed that TGF-β1 stimulation notably accelerated the migration rate of *in vitro*-cultured PSFs ($p < 0.01$). This migration was effectively and dose-dependently suppressed by Binimetinib (Fig. 1C). The significance of this inhibition in the Binimetinib 20 μM group was statistically significant ($p < 0.01$).

Binimetinib Inhibits TGF-β1-Induced Activation of Primary Skin Fibroblasts in Mice

PSFs cultured *in vitro* were treated with TGF-β1 along with different doses of Binimetinib to investigate the drug's impact on cellular fibrogenic factors. As depicted in Fig. 2B, Binimetinib effectively reversed the TGF-β1-induced increase in α-SMA, Col1, and Fn protein levels in a dose-dependent manner (Binimetinib 20 μM, $p < 0.0001$). Concurrently, Binimetinib significantly suppressed the expression of the *α-SMA* gene, as shown in Fig. 2A (Binimetinib 20 μM group, $p < 0.0001$). These findings align with the patterns observed in protein expression. Given the pivotal role of the TGF-β1 signaling pathway in dermal fibrosis progression and the downstream effect of TGF-β1 on recombinant SMAD family member (Smad) 2/3, these findings provide valuable insights into the therapeutic potential of Binimetinib in modulating this pathway and effectively managing conditions associated with dermal fibrosis. Our study investigated the impact of Binimetinib on Smad2/Smad3 activation and its effect on TGF-β1/non-Smad signaling pathways. The findings indicate that treatment with Binimetinib led to a significant increase in the phosphorylation levels of Smad2/3, extracellular regulated protein kinases (ERK), protein kinase B (Akt), and P38 mitogen-activated protein kinase (P38) in response to TGF-β1 ($p < 0.01$) while showing a significant dose-dependent downregulation of these proteins (Binimetinib 20 μM group, $p < 0.001$). Notably, there was no significant effect observed on the total protein levels of Smad2/3, ERK, Akt, and P38 in the treated group (Fig. 2C).

Journal of
BIOLOGICAL REGULATORS
and Homeostatic Agents

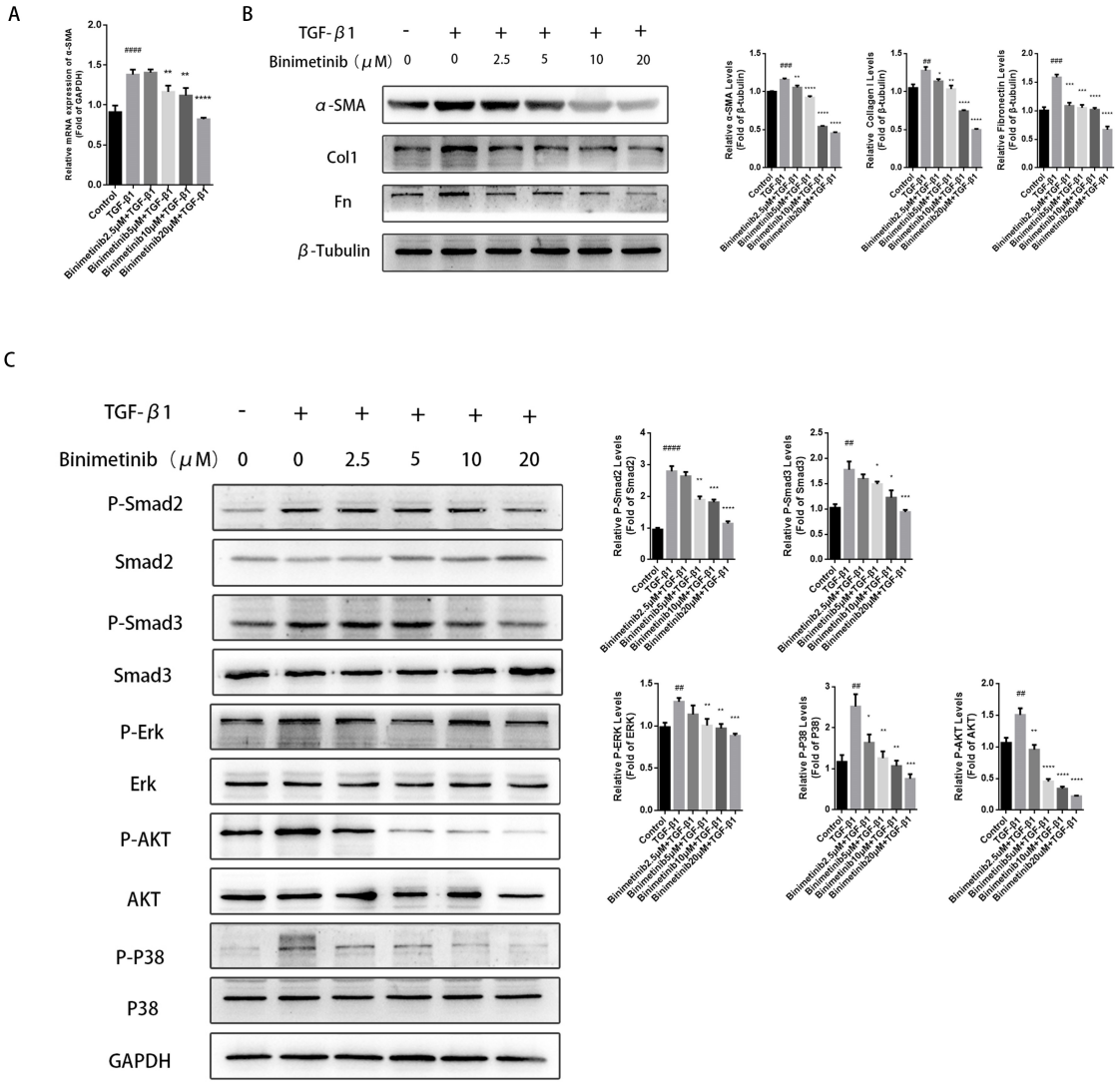

Fig. 2. Binimetinib inhibits the activation of PSFs. (A) Binimetinib inhibits mRNA expression of α-*SMA* in TGF-β1-activated PSFs. (B) PSF cells were exposed to Binimetinib and/or TGF-β1 (5 ng/mL) for 24 h, samples were collected and Western blot assay was performed to detect the protein levels of α-SMA, collagen I, and fibronectin. (C) PSF cells were exposed to Binimetinib for 24 h followed by the addition of TGF-β1 (5 ng/mL), and protein samples were collected after 0.5 h of TGF-β1 action. Western blot was used to detect the effect of Binimetinib on the phosphorylation levels of the TGF-β1/Smad pathway and TGF-β1/non-Smad pathway. The results are expressed as mean ± SD (n = 3). $^{\#}$ represents the difference between Control and TGF-β1 groups, $^{\#\#}p < 0.01$, $^{\#\#\#}p < 0.001$, $^{\#\#\#\#}p < 0.0001$, * represents the difference between TGF-β1 and Binimetinib groups, $^{*}p < 0.05$, $^{**}p < 0.01$, $^{***}p < 0.001$, $^{****}p < 0.0001$.

Binimetinib Inhibits Proliferation, Migration, and Invasion of Keloid Fibroblasts

In a similar context, we investigated whether Binimetinib could effectively impede the growth, movement, and invasion of KFs as it does with PSFs. The impact of Binimetinib on KFs' proliferation was assessed using a CCK-8 kit. The findings revealed a significant dose-dependent suppression of cell proliferation within 24 h in the Binimetinib-treated group compared to the Control group (Fig. 3A). The inhibition observed in the Binimetinib 20 μM group was statistically significant ($p < 0.001$).

Furthermore, in Fig. 3B, the wound healing assay demonstrated that Binimetinib significantly inhibited the migration capacity of KFs in a dose-dependent manner ($p < 0.0001$).

Binimetinib Inhibits Expression in Keloid Fibroblasts Associated with Keloid Pathogenesis

Binimetinib directly affected the pro-fibrotic phenotype of KFs *in vitro*. In Fig. 4A, Binimetinib reduced the mRNA expression levels of Col1, Col3, α-SMA, and Fn in KF cells in a dose-dependent manner, with the Binime-

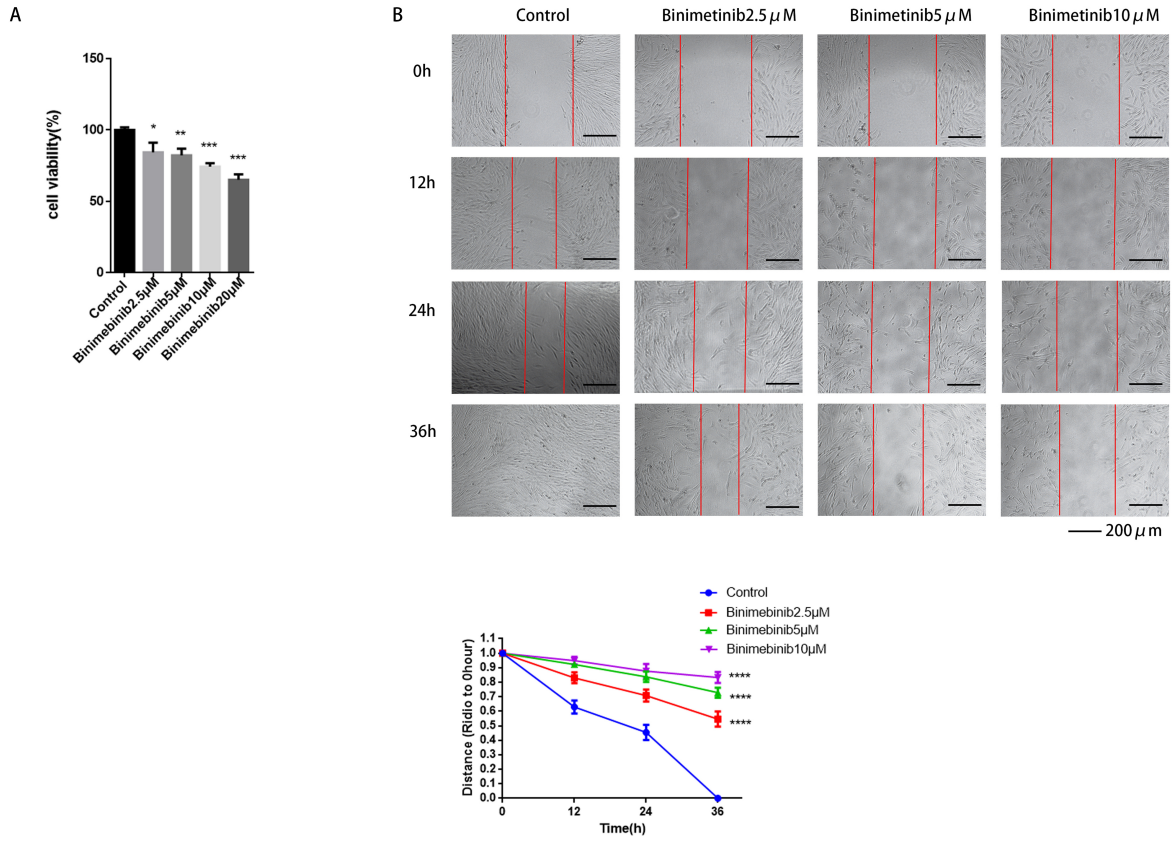

Fig. 3. Binimetinib inhibits the proliferation and migration of KFs. (A) Binimetinib inhibited human keloid fibroblasts proliferation. (B) Wound healing assay. Results are expressed as mean ± SD (n = 3). * represents the difference between Control and Binimetinib groups, *$p < 0.05$, **$p < 0.01$, ***$p < 0.001$, ****$p < 0.0001$. KFs, keloid fibroblasts.

tinib 10 μM group showing statistically significant inhibition ($p < 0.01$). Similarly, immunoblotting experiments showed that Binimetinib significantly reduced the expression levels of α-SMA, Col1, and Fn, with the Binimetinib 20 μM group showing statistically significant inhibition ($p < 0.0001$) (Fig. 4B).

As depicted in Fig. 4C, Binimetinib markedly diminished the phosphorylation levels of Smad2/3 in a dose-dependent manner compared to the Control group. The inhibition observed in the Binimetinib 20 μM group was highly significant at $p < 0.0001$. Additionally, Binimetinib effectively suppressed the phosphorylation of non-classical TGF-β signaling pathways, including ERK, Akt, and P38. The inhibition in the Binimetinib 20 μM group was also statistically significant at $p < 0.001$.

Binimetinib Attenuates BLM-Induced Dermal Fibrosis in Mice and Inhibits Fibrinogen Activation in Vivo

To investigate the effect of Binimetinib on BLM-induced skin fibrosis, C57BL/6 mice received daily subcutaneous injections of BLM and Binimetinib for three weeks. Histological analysis using H&E and Masson trichrome staining of skin tissues revealed that, compared to the model group, the group treated with Binimetinib exhibited a significant, dose-dependent reduction in skin thickness and collagen deposition induced by BLM (Fig. 5A). The inhibition was statistically significant in the Binimetinib 20 μM group ($p < 0.0001$). Furthermore, Binimetinib was effective in reducing hydroxyproline levels in the skin tissues of BLM-treated mice (Fig. 5B). The inhibition was statistically significant in the Binimetinib 20 μM group ($p < 0.01$).

Immunohistochemistry results showed that Binimetinib injection reduced the protein expression of fibrosis makers in BLM-induced skin tissues (Fig. 5C). The inhibitory effect observed in the Binimetinib 20 μM group was statistically significant at a level of $p < 0.01$.

Binimetinib Attenuates Proliferation and Fibrosis in a Subcutaneous Keloid Model in Nude Mice

We injected human keloid fibroblasts into immunodeficient nude mice to simulate the keloid pathological process and administered different drug treatments for one week. The results showed that Binimetinib effectively inhibited keloid proliferation ($p < 0.01$) in this model (Fig. 6A). To explore the underlying molecular mechanisms, we performed Western blot and qPCR experiments, revealing that Binimetinib effectively downregulated the expressions of fibrosis markers α-SMA, Col1, and Fn at both the mRNA ($p < 0.001$) and protein ($p < 0.0001$) levels

Journal of
BIOLOGICAL REGULATORS
and Homeostatic Agents

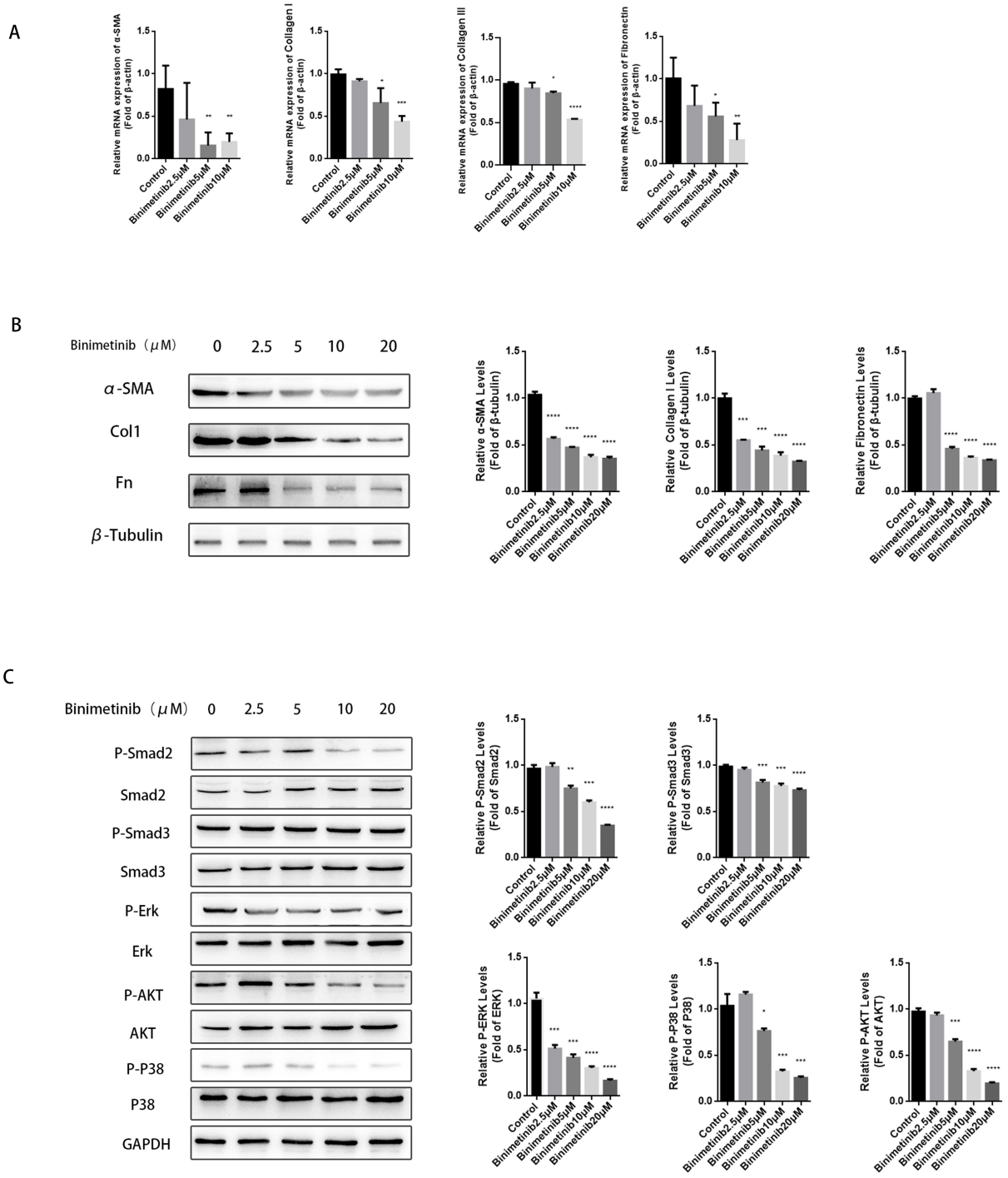

Fig. 4. Binimetinib inhibits the activation of KFs. After KSF cells were treated with Binimetinib for 24 h, samples were collected and subjected to (A) real-time fluorescence quantitative PCR and (B) Western blot assay. The effects of Binimetinib on the expression levels of α-SMA, collagen I, and fibronectin. (C) Western blot assay. The effects of Binimetinib on phosphorylation levels of TGF-β1/Smad pathway and TGF-β1/non-Smad pathway were detected. Results are expressed as mean ± SD (n = 3). * represents the difference between Control group and Binimetinib group, *$p < 0.05$, **$p < 0.01$, ***$p < 0.001$, ****$p < 0.0001$. PCR, Polymerase Chain Reaction.

(Fig. 6B,C). Further investigation revealed that Binimetinib effectively inhibited the phosphorylation levels of Smad2/3 ($p < 0.0001$), ERK ($p < 0.01$), Akt ($p < 0.0001$), and P38 ($p < 0.0001$) in this model (Fig. 6D).

Discussion

Dermatofibrosis is a histopathological condition characterized by excessive proliferation of fibroblasts and deposition of extracellular matrix in the skin [20]. Keloid

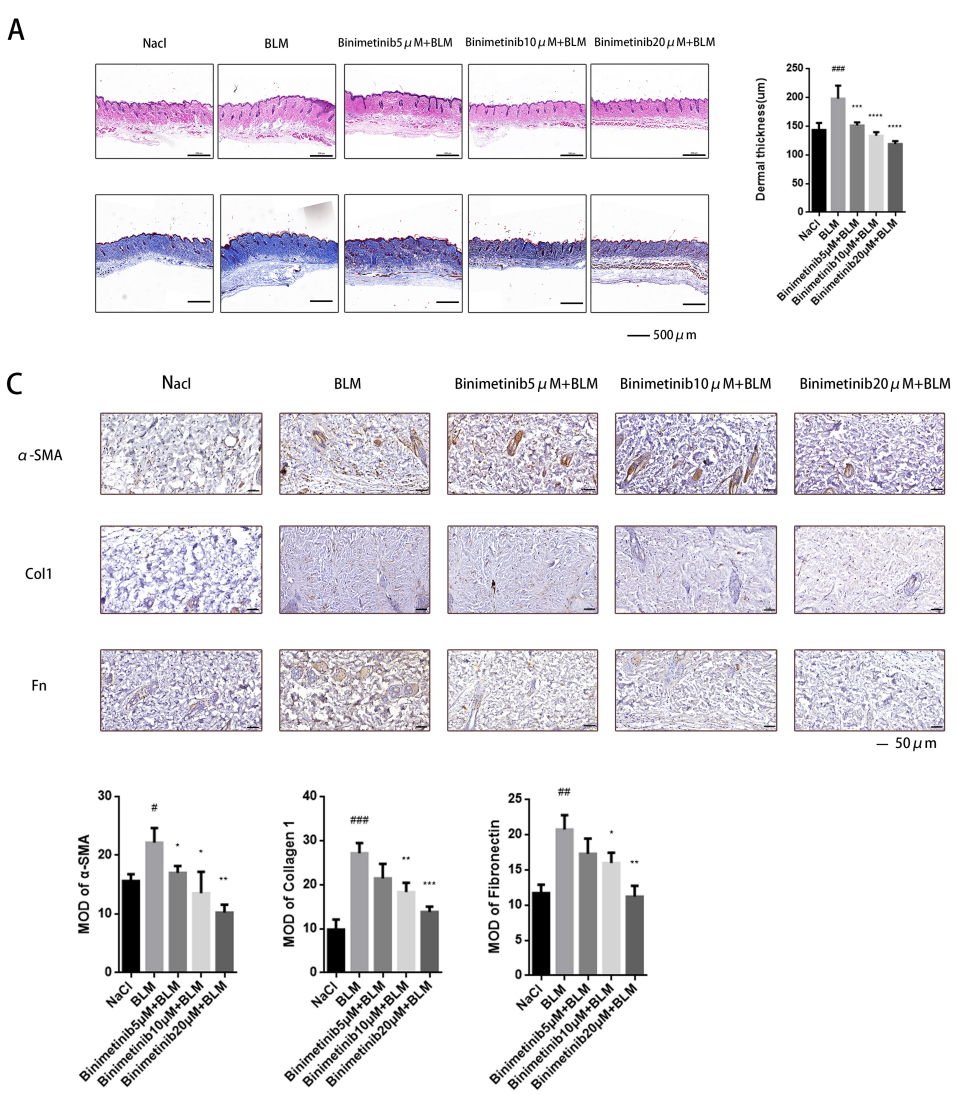

Fig. 5. Binimetinib inhibits fibrosis in the BLM model. (A) H&E and Masson staining results (Scale bar: 500 μm), dermal layer thickness. (B) Effect of Binimetinib on hydroxyproline content of mouse skin tissue. (C) Sections were subjected to immunohistochemical tests (Scale bar: 50 μm) for α-SMA, collagen I, and fibronectin proteins. Results are expressed as mean ± SD (n = 5). $^{\#}$ represents the difference between NaCl group and BLM group, $^{\#}p < 0.05$, $^{\#\#}p < 0.01$, $^{\#\#\#}p < 0.001$. * represents the difference between BLM group and Binimetinib group, $^{*}p < 0.05$, $^{**}p < 0.01$, $^{***}p < 0.001$, $^{****}p < 0.0001$. H&E, hematoxylin and eosin; BLM, bleomycin; MOD, mean optical density.

scarring presents clinical challenges due to its resistance to treatment and tendency to recur easily [21]. Despite significant research efforts to understand the pathogenesis of keloids, only a limited number of interventions and treatments have progressed to clinical trials. This study aimed to explore the potential effects of Binimetinib on dermal fibrosis, investigating its mechanisms both *in vivo* and *in vitro*. *In vitro* experiments demonstrated that Binimetinib effectively inhibits the proliferation, migration, invasion, and activation of dermal fibroblasts, leading to a successful reduction in extracellular matrix deposition. Furthermore, *in vivo* studies demonstrated the efficacy of Binimetinib in reducing dermal fibrosis, as indicated by a significant decrease in scar tissue weight and expression levels of fibrosis markers. These findings provide compelling evidence of Binimetinib's antifibrotic potential, presenting a novel approach for the clinical treatment of dermatofibrotic diseases.

The conventional view of TGF-β signaling suggests that Smad regulates gene expression within the nucleus in a relatively linear manner through receptor complexes located on the plasma membrane. However, emerging evidence indicates that these signaling pathways exhibit more complex networks. Binimetinib is often considered a selective inhibitor of MEK1/2-ERK in the TGF-β1/non-Smad pathway. Our studies show that it also inhibits the MEK3/4-P38 and Akt signaling pathways. Moreover, the inhibitory effect of Binimetinib on the TGF-β1/Smad signaling path-

Journal of
BIOLOGICAL REGULATORS
and Homeostatic Agents

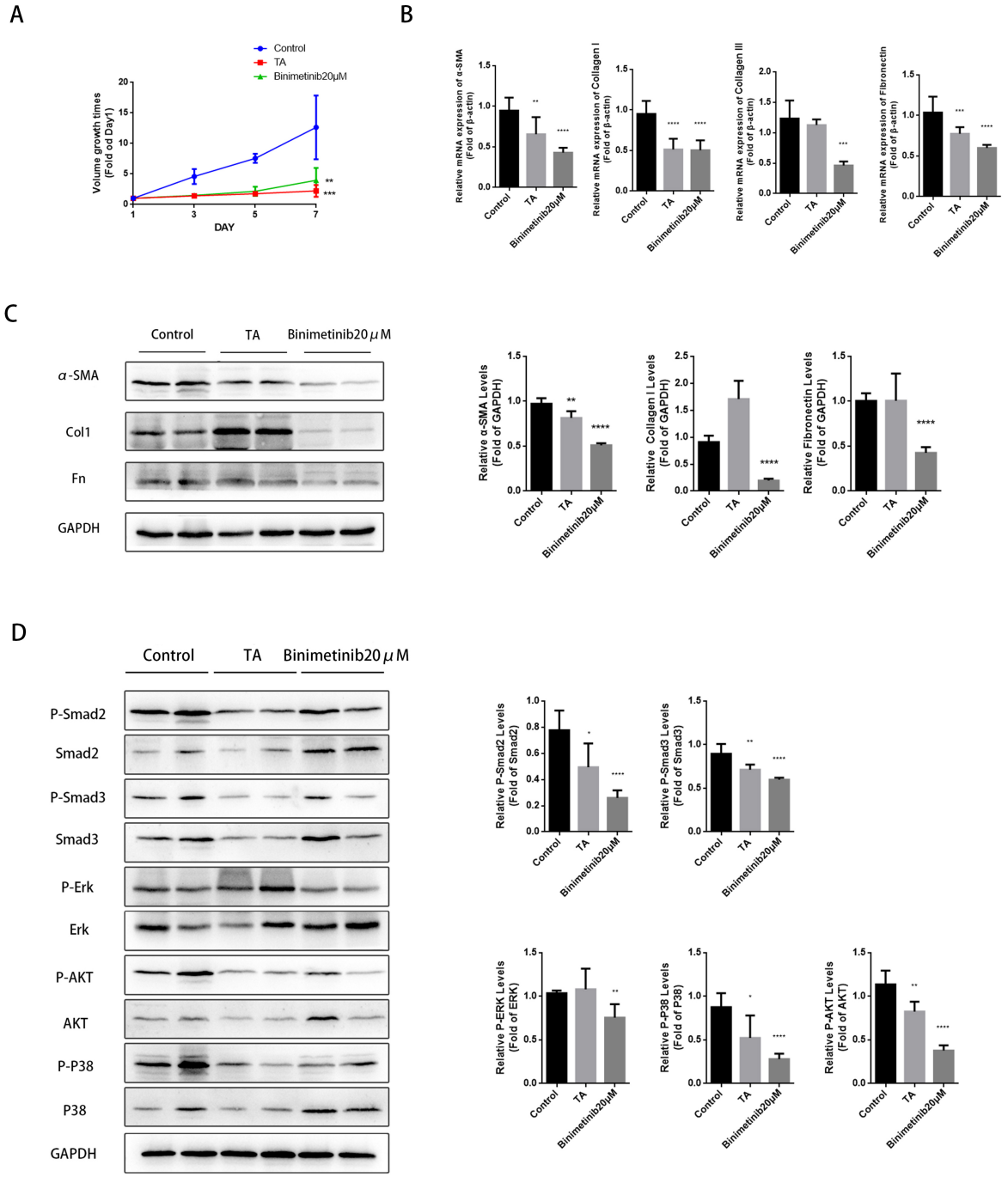

Fig. 6. Binimetinib inhibits fibrosis in a subcutaneous keloid model in nude mice. (A) Keloid volume growth curve. (B) Quantitative Real-Time Polymerase Chain Reaction on tissues to verify the effect of Binimetinib on mRNA levels of fibrosis markers in a nude mouse subcutaneous keloid model. (C) Western blot experiment to verify the effect of Binimetinib on the protein expression of α-SMA, collagen I, and fibronectin in the subcutaneous keloid model of nude mice. (D) Effects of Binimetinib on TGF-β1/Smad and TGF-β1/non-Smad signaling pathways in subcutaneous keloid model in nude mice. Results are expressed as mean $\pm$ SD (n = 5). * represents the difference between the Control group and TA group or Binimetinib group, *$p < 0.05$, **$p < 0.01$, ***$p < 0.001$, ****$p < 0.0001$. TA, triamcinolone acetonide.

way confirms the intricate interconnections between Smad-dependent and Smad-independent signaling pathways of TGF-β1. These connections integrate various signaling pathways into a network that facilitates their interaction and coordination. Binimetinib significantly inhibited several signaling nodes within this network, demonstrating a potent anti-fibrotic capacity.

In this research, a subcutaneous keloid model involving nude mice was created to simulate the progression of human keloids [22]. The results demonstrated that the nude mouse subcutaneous keloid model has the ability of angiogenesis, continuous proliferation, and sustained collagen synthesis. Furthermore, the model can remain active for weeks to months after implantation and continue to grow even after passage. Thus, this model can effectively replicate the characteristics of human keloid tissue. Nonetheless, it is important to note that this model is not without its limitations. While nude mice, lacking a functional thymus, show reduced transplant rejection due to the absence of functional T cells, it is important to note that these thymus-free nude mice still retain a regular innate and humoral adaptive immune system, including operational killer cells. This biological reality is an integral part of their biological makeup and, thus, affects the complete accuracy of simulation scenarios. These immune responses acting on KFs injected into nude mice may affect the viability of the model tissues, thereby influencing the overall validity of the model [23].

Conclusions

To summarize, our study demonstrates that Binimetinib effectively inhibits the proliferation, migration, and activation of PSFs and KFs, and effectively inhibits fibrotic deposition in the skin of bleomycin model mice and proliferation in a nude mouse subcutaneous keloid model. Further studies reveal that Binimetinib suppresses skin fibroblast activation by targeting the TGF-β1/Smad signaling pathway and the non-classical TGF-β pathways including ERK, Akt, and P38. In conclusion, Binimetinib emerges as a promising therapeutic candidate for dermatofibrosis in dermatofibroblastic diseases. This study provides a new idea for mechanism exploration and treatment of keloid and other fibrotic diseases.

Availability of Data and Materials

All experimental data included in this study can be obtained by contacting the first author RS if needed.

Author Contributions

LZ and XL designed the research study. RS performed the research. HZ and LZ provided help and advice on the experiments. RS analyzed the data. RS drafted this manuscript. All authors contributed to important editorial changes in the manuscript. All authors read and approved the final manuscript. All authors have participated sufficiently in the work and agreed to be accountable for all aspects of the work.

Ethics Approval and Consent to Participate

The study's methods were approved by the Ethics Committee of Nankai University on December 20th, 2021 (Approval No. NKUIRB2021116), and all experimental protocols strictly adhered to the appropriate guidelines and regulations about human subjects. Each human participant involved in this research provided their informed consent preceding their enrollment in the study. The animal experiments were conducted with approval from the Institutional Animal Care and Use Committee (IACUC) of Nankai University, under approval number SYXK 2019-0001.

Acknowledgment

Not applicable.

Funding

This study was supported by The Fundamental Research Funds for the Central Universities, Nankai University [Grant 735-ZB23003405], The National Natural Science Foundation of China [Grant 82270069], and Shenzhen Science and Technology Program [Grant JCYJ20210324122006017].

Conflict of Interest

The authors declare no conflict of interest.

References

[1] Eming SA, Martin P, Tomic-Canic M. Wound repair and regeneration: mechanisms, signaling, and translation. Science Translational Medicine. 2014; 6: 265sr6.

[2] Tan S, Khumalo N, Bayat A. Understanding Keloid Pathobiology From a Quasi-Neoplastic Perspective: Less of a Scar and More of a Chronic Inflammatory Disease With Cancer-Like Tendencies. Frontiers in Immunology. 2019; 10: 1810.

[3] Mutalik S. Treatment of keloids and hypertrophic scars. Indian Journal of Dermatology, Venereology and Leprology. 2005; 71: 3–8.

[4] Moretti L, Stalfort J, Barker TH, Abebayehu D. The interplay of fibroblasts, the extracellular matrix, and inflammation in scar formation. The Journal of Biological Chemistry. 2022; 298: 101530.

[5] Deng CC, Hu YF, Zhu DH, Cheng Q, Gu JJ, Feng QL, *et al*. Single-cell RNA-seq reveals fibroblast heterogeneity and increased mesenchymal fibroblasts in human fibrotic skin diseases. Nature Communications. 2021; 12: 3709.

[6] Chen CJ, Kajita H, Takaya K, Aramaki-Hattori N, Sakai S, Asou T, *et al*. Single-Cell RNA-seq Analysis Reveals Cellular Functional Heterogeneity in Dermis Between Fibrotic and Regenerative Wound Healing Fates. Frontiers in Immunology. 2022; 13: 875407.

[7] Penn JW, Grobbelaar AO, Rolfe KJ. The role of the TGF-β family in wound healing, burns and scarring: a review. International Journal of Burns and Trauma. 2012; 2: 18–28.

[8] Zhang T, Wang XF, Wang ZC, Lou D, Fang QQ, Hu YY, *et al*. Current potential therapeutic strategies targeting the TGF-β/Smad signaling pathway to attenuate keloid and hypertrophic

Journal of
BIOLOGICAL REGULATORS
and Homeostatic Agents

scar formation. Biomedicine & Pharmacotherapy. 2020; 129: 110287.

[9] Chalmers RL. The evidence for the role of transforming growth factor-beta in the formation of abnormal scarring. International Wound Journal. 2011; 8: 218–223.

[10] Zehender A, Li YN, Lin NY, Stefanica A, Nüchel J, Chen CW, *et al*. TGFβ promotes fibrosis by MYST1-dependent epigenetic regulation of autophagy. Nature Communications. 2021; 12: 4404.

[11] Woodfield SE, Zhang L, Scorsone KA, Liu Y, Zage PE. Binimetinib inhibits MEK and is effective against neuroblastoma tumor cells with low NF1 expression. BMC Cancer. 2016; 16: 172.

[12] Dong J, Li S, Liu G. Binimetinib Is a Potent Reversible and Time-Dependent Inhibitor of Cytochrome P450 1A2. Chemical Research in Toxicology. 2021; 34: 1169–1174.

[13] Jumper N, Paus R, Bayat A. Functional histopathology of keloid disease. Histology and Histopathology. 2015; 30: 1033–1057.

[14] Li X, Zhai Y, Xi B, Ma W, Zhang J, Ma X, *et al*. Pinocembrin Ameliorates Skin Fibrosis via Inhibiting TGF-β1 Signaling Pathway. Biomolecules. 2021; 11: 1240.

[15] Tucci-Viegas VM, Hochman B, França JP, Ferreira LM. Keloid explant culture: a model for keloid fibroblasts isolation and cultivation based on the biological differences of its specific regions. International Wound Journal. 2010; 7: 339–348.

[16] Li X, Fang Y, Jiang D, Dong Y, Liu Y, Zhang S, *et al*. Targeting FSTL1 for Multiple Fibrotic and Systemic Autoimmune Diseases. Molecular Therapy. 2021; 29: 347–364.

[17] Rinkevich Y, Walmsley GG, Hu MS, Maan ZN, Newman AM, Drukker M, *et al*. Skin fibrosis. Identification and isolation of a dermal lineage with intrinsic fibrogenic potential. Science. 2015; 348: aaa2151.

[18] Kim B. Western Blot Techniques. Methods in Molecular Biology. 2017; 1606: 133–139.

[19] Choi MH, Kim J, Ha JH, Park JU. A selective small-molecule inhibitor of c-Met suppresses keloid fibroblast growth *in vitro* and in a mouse model. Scientific Reports. 2021; 11: 5468.

[20] Ho YY, Lagares D, Tager AM, Kapoor M. Fibrosis–a lethal component of systemic sclerosis. Nature Reviews. Rheumatology. 2014; 10: 390–402.

[21] Al-Attar A, Mess S, Thomassen JM, Kauffman CL, Davison SP. Keloid pathogenesis and treatment. Plastic and Reconstructive Surgery. 2006; 117: 286–300.

[22] Wang M, Chen L, Huang W, Jin M, Wang Q, Gao Z, *et al*. Improving the anti-keloid outcomes through liposomes loading paclitaxel-cholesterol complexes. International Journal of Nanomedicine. 2019; 14: 1385–1400.

[23] Rolstad B. The athymic nude rat: an animal experimental model to reveal novel aspects of innate immune responses? Immunological Reviews. 2001; 184: 136–144.